# A Low Sample Rate Real Time Advanced Sonar Ring

**Saeid Fazli and Lindsay Kleeman**
**ARC Centre for Perceptive and Intelligent Machines in Complex Environments (PIMCE)**
**Intelligent Robotics Research Centre(IRRC)**
**Monash University, Australia**
**Saeid.fazli@eng.monash.edu.au**
**Lindsay.kleeman@eng.monash.edu.au**

## Abstract

This paper describes an *advanced sonar ring* that employs a low receiver sample rate to achieve processing of 48 receiver channels at near real time repetition rates of 15 Hz. The sonar ring sensing covers 360 degrees around the robot with simultaneously firing of 24 transmitters. The receiver sampling frequency is 250 kHz, compared to previous work at 1 MHz, firstly to maximize the speed of processing and secondly to avoid memory limitations of the DSPs. The processing to produce accurate distance and bearing measurements is performed on 6 DSPs using template matching of echoes with short duration. This paper presents a summary of the hardware architecture, software architecture and sensing theory of the *advanced sonar ring*. The use of a reference point and offset table is introduced and experimentally verified to improve the sensor accuracy and robustness. The problem and solution to cycle hopping, caused by the low sampling rate, are described in the paper.

## 1 Introduction

A fast, accurate and robust environment sensor is always a critical part of robotic tasks such as map building, localization, target tracking and collision avoidance. As research in this area increases, the accuracy of sonar sensors has improved [Peremans, Audenaert et al. 1993; Kleeman and Kuc 1995; Joerg and Berg 1998; Kleeman 1999; Yata, Ohya et al. 1999; Yata, Ohya et al. 2000].

Meanwhile, Digital Signal Processor (DSP) systems have enabled the ultrasonic echo to be sampled at 12 bit amplitude resolution and 1 MHz sample rate and then processed in near real time to measure range to 0.2 mm and bearing to 0.1 degrees [Heale and Kleeman 2000]. This approach is fast and accurate but operates only within the beamwidth of the transducers. Mechanical scanning and many measurements taken in sequence are needed to cover a full 360 degrees.

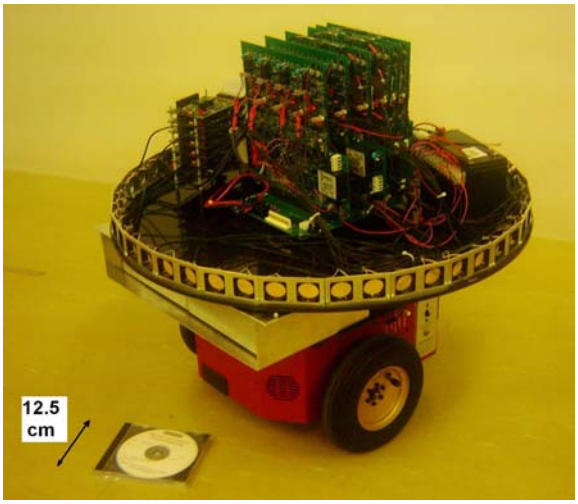


Figure 1. Advanced sonar ring mounted on an ActivMedia Pioneer 3 DX mobile robot.

The sonar ring makes possible rapid navigation of a mobile robot without the complication of mechanical scanning and delays associated with scanning sensors, such as scanning laser or sonar [Vlastimil MASEK 1998; Vlastimil MASEK 1999].

Researchers have developed a sonar ring that allows simultaneous firing of transmitters and thresholding of echo signals to measure reflectors with a bearing accuracy of around 1 degree [Yata, Ohya et al. 1999; Yata, Ohya et al. 2000]. Furthermore, interference can be rejected [Borenstein and Koren 1995; Joerg and Berg 1998; Kleeman 1999], making possible the operation of multiple sonars in the same acoustic space, or in noisy spaces. This is important for cooperative robotics, swarm robotics or any time two sonar equipped mobile robots that need to work in the same area.

The increasing performance of DSPs makes it possible to perform intensive sonar echo processing around an entire ring of 48 transducers from a single simultaneous set of transmissions in near real time. Thus the sequential scanning of the individual sonar sensors has been condensed into one measurement cycle. The new real time multi-DSP advanced sonar ring is first reported in [Fazli and Kleeman 2004] and this paper discusses low sample rate issues and solutions to cycle hopping.

The sample rate of the advanced sonar ring is as low as 250 KHz , allowing each DSP to process all echoes of 8 receivers in near real time and save all processed information in the memory of each DSP which is 192 KB. A low sample rate gives rise to problems, such as lower accuracy and cycle hopping that may cause stationary targets to appear to shift in bearing and hop a wavelength in range.

The next section briefly introduces hardware components of the advanced sonar ring. The sensing theory, known as matched filtering, is presented in section 3. This section shows that the maximum likelihood estimator of the arrival time of the echo corrupted by additive white Gaussian noise is the best estimator [P.M.Woodward 1964]. This theory is important for understanding and solving the problem of cycle hopping discussed later.

Section 4 briefly introduces the advanced sonar ring software architecture and the implementation of pulse capturing and storing within a DSP context. Experimental results are presented in section 5 to show the effectiveness of the proposed system. In this section the concept of cycle hopping rejection is explained. Conclusions are presented in the last section.

## 2 The Advanced Sonar Ring Hardware Architecture in Brief

Figure 1 shows the advanced sonar ring mounted on an ActivMedia Pioneer 3 DX mobile robot. It contains a 48-transducer sonar ring, each group of eight Polaroid 7000 series transducers, arranged in four pairs, controlled by a digital slave DSP board and an associated analogue board. Each pair consists of a transceiver and a receiver 40 mm and 15 degrees apart. The sensor is capable of covering a full 360 degrees around robot when the effective beamwidth of each pair of transducers is at least 15 degrees and this occurs for highly reflective specular targets at ranges closer than 2.8 m.

The advanced sonar ring has six analogue slave PCBs which are responsible for simultaneous firing of all transmitters and data acquisition process. Each of them is controlled by a digital slave board containing a DSP. The receiver channels are amplified and low pass filtered before sampling with ADCs at 250 kHz. The transmission electronics allow a programmable digital pulse train to be sent to the transducer without the need for preloaded memory buffers. Instead the digital slave DSP directly controls the transmit logic every microsecond under interrupt service routine. Variable gain amplifiers control the amplitude of the received echoes from different ranges. Also each board contains a high voltage DC-DC converter to produce a 300 V bias on the 8 transducers (Figure 2).

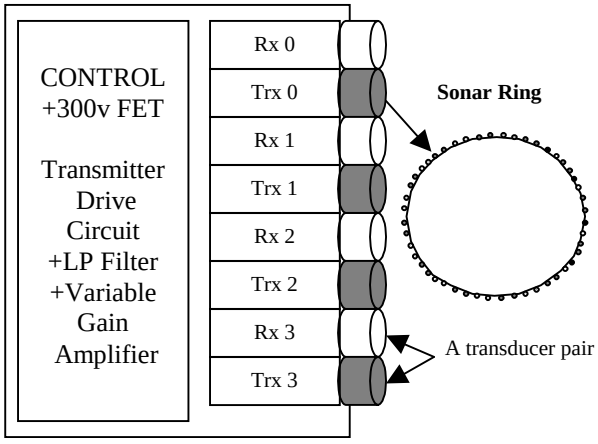


Figure 2. A Sonar Ring and an Analogue Slave PCB Block Diagram

After pulses are transmitted and echoes are captured by analog slave, the echoes are digitized by Analog to Digital Converters (ADC) of digital slave boards. The sensor has six digital slave PCBs, each one contains a DSP which controls an associated analog slave and connects to it using a ribbon cable. The DSP is responsible for generating the transmit pulses for the four transceivers and processing the echoes collected by the eight transducers. Two 12-bit ADS7862 ADCs are configured to allow pairwise synchronised sampling of 8 input channels at 250 kHz sample rate. An Analog Devices 2189M DSP was chosen due to the single clock cycle access to on-chip RAM of 192 k bytes, allowing echoes to be extracted, stored and processed within the DSP chip. The speed of the on-chip memory allows the processor to fetch two operands (one from data memory and one from program memory) and an instruction (from program memory) in a single cycle (Figure 3).

A master PCB controls all six digital slaves and connects the sensor to a host computer. The master board contains a

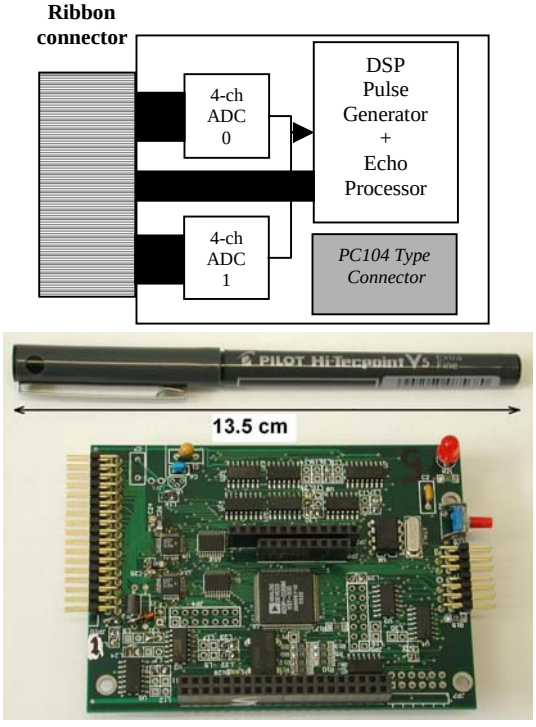


Figure 3. A Digital Slave PCB

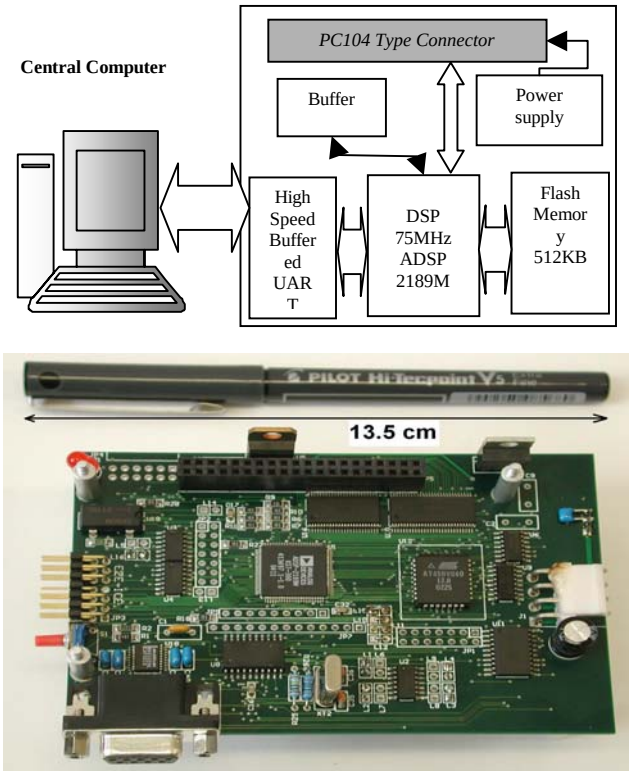


Figure 4. A Master PCB

2189M DSP, flash memory and a high speed buffered UART (Figure 4). It communicates with a central computer via the high speed serial link and with all the digital slave boards via a PC104 type connector using the Internal Direct Memory Access (IDMA) port. The DSPs contain two DMA ports, Internal DMA port and Byte DMA port. The IDMA port provides an efficient means of access the on-chip program memory and data memory of the DSP with only one cycle per word of overhead. The IDMA port has a 16-bit multiplexed address and data bus and supports 24-bit program memory. The IDMA port is completely asynchronous and can be written to while the ADSP 2189M is operating at full speed. Also, the master board contains the software in the flash memory, boots all the slave DSPs using BDMA port, sends all user commands and reads the high level data from slave boards and transfers them to a host computer using a RS232 serial port.

## 3 The Advanced Sonar Ring Sensing Theory

The basic idea of range finding is to calculate the Time-Of-Flight (TOF) of captured echoes using matched filtering method based on the radar reception theory. In this section we show that this method is the best arrival time estimator in theory. Equations (1-6) are based on [P.M.Woodward 1964] and justify the optimality of the arrival time estimation used in the advanced sonar ring.

The problem is to extract the information from a noisy received signal. We assume that the wanted information in the receiver is $x$, noise is white Gaussian and the received signal is denoted by $y$. The signal $y$ is available and we require the probability distribution $p(x|y)$, which gives us some information about $x$ from the knowledge of $y$.

The calculatation of $p(x|y)$ is a problem of inverse probability. The product law for probabilities is

$$p(x,y) = p(x)p(y|x) = p(y)p(x|y) \quad (1)$$

and since $y$ is given, the second of these equations may be written

$$p(x|y) = k \; p(x)p(y|x) \quad (2)$$

where k is the normalizing constant of distribution. In equation (2) $p(x)$ is the prior probability of $x$ and $p(x|y)$ is the posterior probability of $x$.

If we denote $u_x$ as a time-dependent signal representing the information $x$ and $n$ as additive white Gaussian noise, then the received waveform is

$$y = u_x + n \quad (3)$$

which is available in the receiver and the reception method should determine $p(x|y)$.

The Likelihood Function is written as

$$p(y|x) = k\exp(-E/N_0) = k\exp\{-\frac{1}{N_0}\int (y-u_x)^2 dt\} \quad (4)$$

where $N_0$ is N/W, N is the mean noise power and W is the bandwidth of the signal. The integral in the equation is definite and the limits must correspond to the total interval of time occupied by the signal. The term $y^2$ can be absorbed into k

$$p(x|y) = k \; p(x)\exp\{-\frac{1}{N_0}\int {u_x}^2 dt\}\exp\{\frac{2}{N_0}\int yu_x dt\} \quad (5)$$

Equation (5) shows that the term

$$q(x) = \int yu_x dt \quad (6)$$

is the only term that depends on $y$ and using that we can obtain all information about posterior distribution.

Equation (6) is a cross correlation between the received signal, y and a predicted noiseless received signal, $u_x$.

In discrete form, equation (5) becomes:

$$p(x|y) = kp(x)\exp\{-\frac{1}{N_0}\sum_t {u_x}^2\}\exp\{\frac{2}{N_0}\sum_t yu_x\} \quad (7)$$

Now let us continue with the problem of range finding or TOF estimation. The pulse shape will be denoted by $u(t)$, a delay of $\tau$ occurs in the pulse shape and the goal is to estimate the value of $\tau$ by analysis of the received waveform $y(t)$, given by

$$y(t) = u(t-\tau) + noise \quad (8)$$

A copy of $u(t)$, as a template, is available for comparison with $y(t)$ at the receiver. It is assumed that $\tau$ is independent of time which means the target is stationary, and also it will be assumed that all the noise in the system, including that which is introduced by the receiver itself while operating on $y(t)$, can be regarded as an addition to the input signal.

Equations (7) can be rewritten as

$$p\ (\tau \mid y) = kp(\tau)\exp\{-\frac{1}{N_0}\sum_t u^2(t-\tau)\}\exp\{\frac{2}{N_0}\sum_t y(t)u(t-\tau)\} \quad (9)$$

Equation (9) shows that to estimate the delay, it is sufficient to calculate the convolution of $y(t)$ and $u(-t)$ - that is a cross correlation. None of the remaining terms involve $y(t)$.

The importance and effectiveness of cross correlation is shown in Figure 5. Figure 5 (a) shows a typical sample of Gaussian noise. The noise was constructed using a random function. The signal chosen is shown in Figure 5 (b) which is real data captured by advanced sonar ring. As shown in the figure, $u(t)$ is delayed by an amount $\tau_0$ which represents the TOF for the target. The sum of noise and signal, $y(t)$, is shown in Figure 5 (c). $u(t)$ and $y(t)$ are available at the receiver, but $u(t-\tau_0)$ as shown if Figure 5 (b), is not. The problem is to estimate where $u(t)$ is located in the noise.

Estimation process starts with

$$q(\tau) = \frac{2}{N_0}\sum_t y(t)u(t-\tau) \quad (10)$$

$q(\tau)$ has been computed over as wide range as possible, as shown in Figure 5 (d). It will be seen that $q(\tau)$ has reduced the bandwidth of the noise so that it has a similar structure to that of the signal . In fact, this is because of cross-correlation process, which is an effective filter.

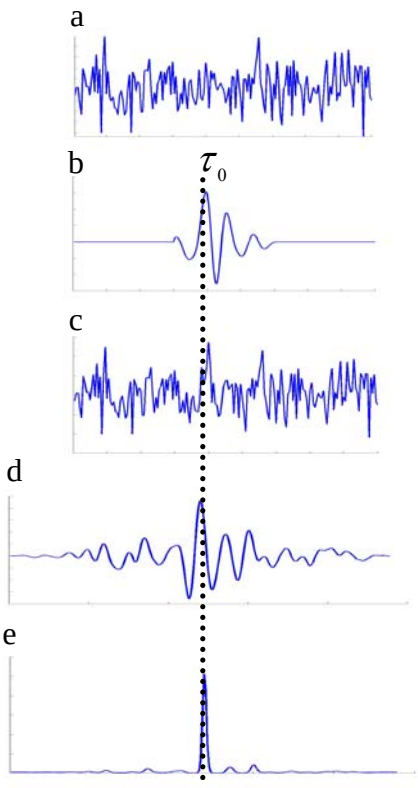


Figure 5. (a) Gaussian noise, (b) signal at t= $\tau_0$, (c) noise + signal, (d) $q(\tau)$, (e) posterior distribution for $\tau$ (Note: The length of the signals d and e are bigger than a,b and c due to the croos correlation)

In Figure 5 (e), the exponential function of $q(\tau)$ is plotted against $\tau$, and if the prior distribution $p(\tau)$ is uniform, this final graph represents the complete expression (9) for $p\ (\tau \mid y)$.

It will be seen that all the posterior probability is concentrated in a narrow region of uncertainity at approximately the true value of $\tau$. Actually, due to sampling effects and noise, the maximum of $p\ (\tau \mid y)$ does not fall exactly at the true value shown in Figure 5 (b). In fact, one of the important factors in this process is signal/noise energy ratio that affects the uncertainity of the delay estimation.

Now, we describe the application of this method in the advanced sonar ring. The sonar ring simultaneously fires all 24 transmitters of the ring using a very short square-wave pulse, and analyses simultaneously the waveforms of all 48 receivers using matched filters to accurately determine the arrival time of echoes.

The transmitted pulse is 2 cycles of 71.4 kHz plus a counter-timed burst to reduce reverberation in the transducer. The pulse is generated by momentarily removing a 300V bias, the same bias as is required to operate the transducers as receivers. Figure 6 shows the voltage waveform used to drive transmitters, a sample waveform received from a smooth, hard reflector and the frequency components of the echoed signal using fast Fourier transform (FFT) .

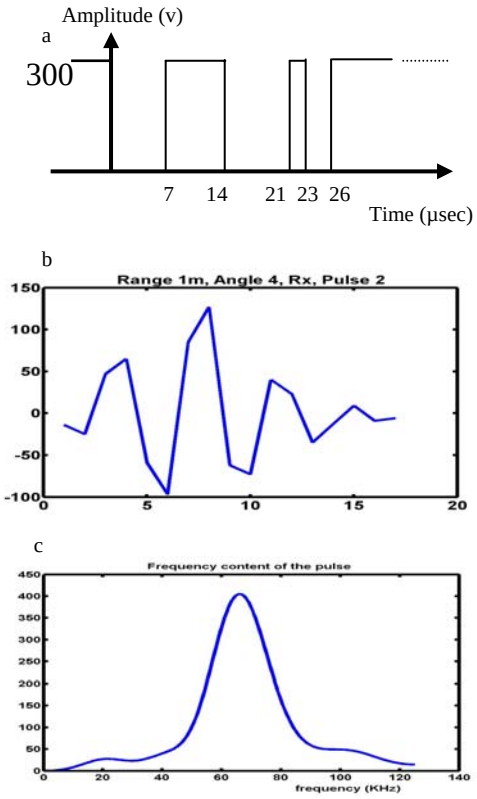


Figure 6. (a) voltage waveform to drive transmitters (b) an echo (c) frequency components of the echo

A template for one metre range and zero bearing was used as a prototype, and physical models used by [Kleeman and Kuc 1995] were applied to generate the templates shown. The pulse absolute amplitude is normalised to maximum of 127, so the waveforms can be stored in an array of signed bytes. Multiple matched filters are required to maintain accuracy because the pulse shape depends greatly on the bearing of the reflector and its range.

Due to different electronic circuits applying to transceivers and receivers of the advanced sonar ring, the echo pulse shapes of the same target are slightly different and therefore it is necessary to make particular sets of templates for each of them to gain the highest cross correlation.

Because pulse shape depends on range and angle of arrival, several filters are generated. The templates are pre-computed and saved in the DSPs. Finally 13 templates for each set are generated for varying ranges and angles that includes for one metre range, one, four, seven and ten degrees bearing, for two metre range, one, four and eight degrees bearing, for three metre range, two and six degrees bearing, for four metre range, two and six degrees bearing and for five metre range, two and six degrees bearing.

Based on above mentioned theory, the maximum likelihood estimator for the arrival TOF with additive white Gaussian noise is the time $\tau$ that maximizes the cross-correlation, $Cor(\tau)$, between the received pulse $p(t)$ and an anticipated pulse shape $ant(t)$.

$$Cor(\tau) = \frac{\sum_{T} p(t)ant(t-\tau)}{\sqrt{\sum_{T} p^2(t) \sum_{T} ant^2(t)}} \qquad (11)$$

The anticipated pulse shape $ant(t)$ is one of the templates captured from a plane in one metre range and one degree bearing. The received echo is tried against all available templates for several different angles at the given range, and the one which gives the highest correlation coefficient is selected to estimate the arrival time. A sonar pulse is registered if its maximum cross-correlation is greater than 80% otherwise is discarded. There are some reasons why a pulse may be rejected including environmental noise, another sonar sensor using a different pulse shape, another transmitter in the same sonar ring using different pulse shape or overlapping pulses from different sources, resulting a distorted pulse.

To estimate the TOF to sub-sample accuracy (less than 4 microseconds in the advanced sonar ring), parabolic interpolation is performed on the maximum three adjacent samples of $Cor(\tau)$. If the three maxima y0, y1, and y2 occur at integer sample numbers 0, 1 and 2, the parabolic estimate of the position of the maximum is

$$new\_\max\_pos = prev\_\max\_pos - 1 + \frac{y_2 - 4y_1 + 3y_0}{2(y_2 - 2y_1 + y_0)} \qquad (12)$$

where $prev\_\max\_pos$ is the position of *y1* and $new\_\max\_pos$ is the new maximum position with sub-sample resolution.

TOF is determined by applying matched filtering to the echoes identified by thresholding and pulse splitting. Filtering is performed by first choosing a set of appropriate templates using the start sample number of the echo and finding the approximate range of the echo, then cross correlating the received echo with all selected templates. For example if the start sample number of the echo shows an approximate range of 120 cm, the first four templates are chosen by software. The alignment between the echo and each template are adjusted by 13 samples which means alignment of the peaks on each other and six shifts to each side. This is less comprehensive than a full convolution implementation but is advantageous as it can run faster and because each DSP processes all echoes of eight receivers, the process is computationally intensive.

After finding a reliable echo, exceeding the correlation threshold, which is 80%, the question is how to calculate the TOF. In fact, the TOF is the start point of the echo pulse, but noise can change the start point of the echo and more importantly in practice the thresholding and splitting process, as are explained later, relies on groups of eight samples that at least one of them exceeds the threshold level, therefore the registered start point of the echo varies with time and cannot be considered as a reliable TOF.

The method used in the advanced sonar ring is to find the start point of the template when the alignment of template and pulse results in the maximum correlation.

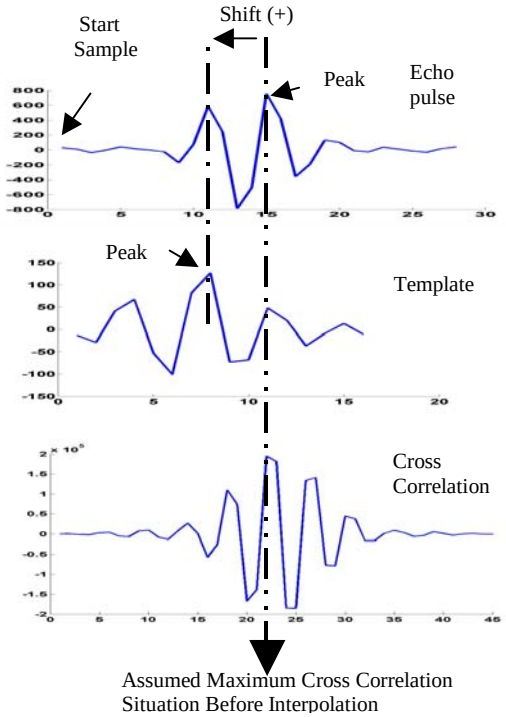


Figure 7. Alignment of a Received Echo and a Template when Maximum Correlation Occurs

Figure 7 shows an example of filtering, which is assumed that maximum correlation happens in the shown condition, , therefore the TOF is

$$TOF = 4\mu\sec(pulse\_peak\_no - template\_peak\_no - shift) \quad (13)$$

where $pulse\_peak\_no$ is sample number of the pulse peak and $template\_peak\_no$ is the sample number of the template peak, and in the calculation of the $shift$, sub sample resolution is considered using equation (12).

$$shift = peak\_dif - (-1 + \frac{y_2 - 4y_1 + 3y_0}{2(y_2 - 2y_1 + y_0)}) \quad (14)$$

where $peak\_dif$ is difference between $pulse\_peak$ and $template\_peak$ when maximum correlation occurs (Figure 7).

## 4 The Advanced Sonar Ring Sofware Architecture in Brief

The software consists of three parts, a host program, a master program and a slave program. The host program is developed using C++ under Linux which provides a graphical user interface to communicate with the sensor using a serial port, and to save the results while showing them in the screen. A user is able to send different commands to the sensor, such as upload and download of data memory and program memory of master DSP and slave DSPs, firing of transducers, reading and writing of the flash memory and transferring the high level data to the host, shown in the graphical environment.

The master and slave programs are stored in the flash memory. After turning on the sensor, the master is booted via the byte DMA method of ADSP-2189M. This software is a command parser capable of communication with the host computer and all digital slave boards, allowing the central computer to control all parts of the advanced sonar ring. By sending a command to the master, it can boot all digital slave boards using internal DMA port. A fire command is issued to all slaves simultaneously, thus synchronizing the firing of all transceivers to within a clock cycle or 13 nanoseconds. The software of each slave can communicate with the master by a command parser containing some commands to access low level data.

The most important part of this software is an echo processor that is organised into two stages. During the first stage, assembly code performs on-the-fly processing of the samples from the eight receivers to extract discrete pulses that exceed the noise floor. On-the-fly processing is essential not only to have a real time sensor but also to conserve the on-chip data memory of the DSP. The second stage processes the extracted pulses with C code to extract arrival times and bearing information using template matching method.

The pulse capturing program consists of optimised assembly code to extract pulses from eight receiver channels and save them into pulse buffers. This real time program enables approximately 128k words of raw receiver data to be processed in a transmit cycle to yield pulse results within the 48k words of data memory. The software is run while receiving echoes and processes all eight channels within 150 instruction cycles or two microseconds.

The eight channels are processed independently through four stages containing DC bias removal, thresholding, aggregation and storing into a pulse buffer. A block processing technique is used for thresholding. Each block of eight samples containing at least one sample with amplitude greater than the threshold are deemed to be part of an echo. When there are two or more consecutive blocks exceeding the threshold level, the software merges them and if there is just a block of 8 samples, the software discards them because each echo must have at least 16 samples (Figure 8). Also, an adaptive threshold level is applied to allow for different time varying gains in the receiver preamplifiers resulting in different noise levels.

Stage two processing occurs in the DSP after all receiver channels have been logged and stored simultaneously in the pulse buffers.

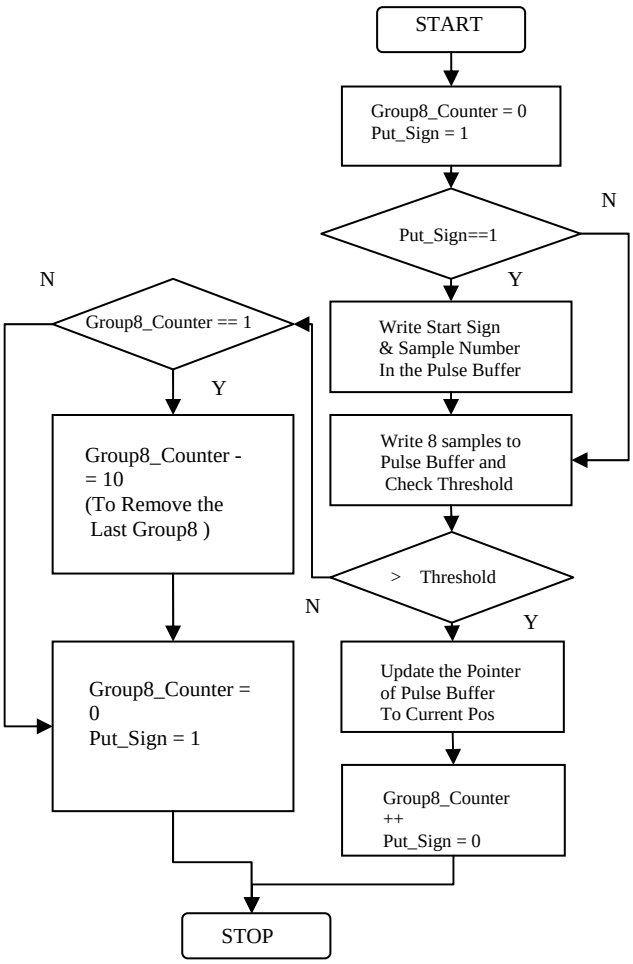


Figure 8. A Flow Chart of an On-The-Fly Thresholding , Aggregation and Storing Assembly Code Running in 150 Instruction Cycles

The processing time in this stage occurs in addition to the time of flight between transmitting and receiving the furthest echo – approximately 32 milliseconds. This processing time then directly impacts on the real time performance of the sensor since it takes place sequentially with respect to the capture time.

To determine the echo pulse arrival times, the above mentioned matched filtering technique is performed on the echo pulses extracted during stage one of the processing.

After all arrival times are estimated, the bearing estimation is performed for all targets seen by both receivers of each pair using a triangulation method. If a target is seen by just one of the receivers it is deemed to be an unreliable target. At the end of the calculation, the slave boards are waiting to be read by the master board and after the high level data of all slave boards are read and sent to the central computer, the master board sends another fire command simultaneously to all the slave boards.

# 5 Experimental Results

## 5.1 Reference Point and Offset Table Concept and Results

Choosing a reference template amongst all precomputed templates is an important issue, which results the exclusive indication of the start point of an echo, matched with varying templates, that is the same TOF when maximum correlation occurs in different templates.

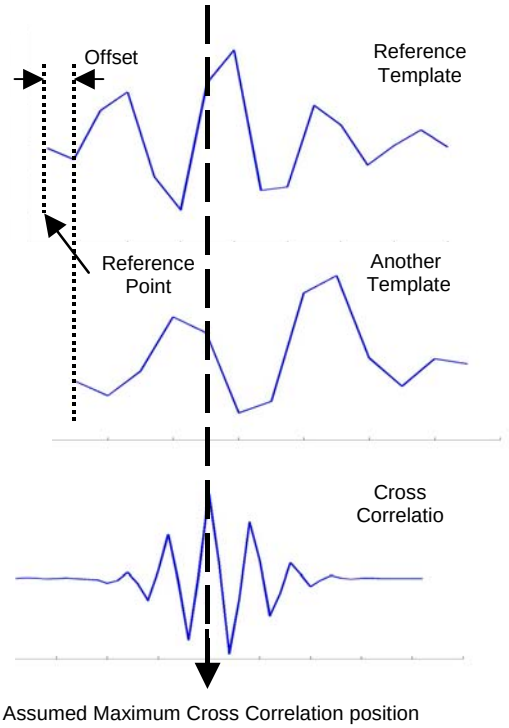


Figure 9. The Concept of the Offset and Calculation Method

The importance is due to varying sizes and asymmetric pulse shapes of templates used in matched filtering. In other words, the TOF of a stationary target or a very slow object, when maximum correlation occurs with different templates in matched filtering, in the templates of the same range or different ranges, is varying because of the different start points of templates.

In the advanced sonar ring, to solve this problem and avoid jumping TOFs, the template for one metre range and one degree bearing is selected as reference template and the start point of that is considered as the reference point of echoes .

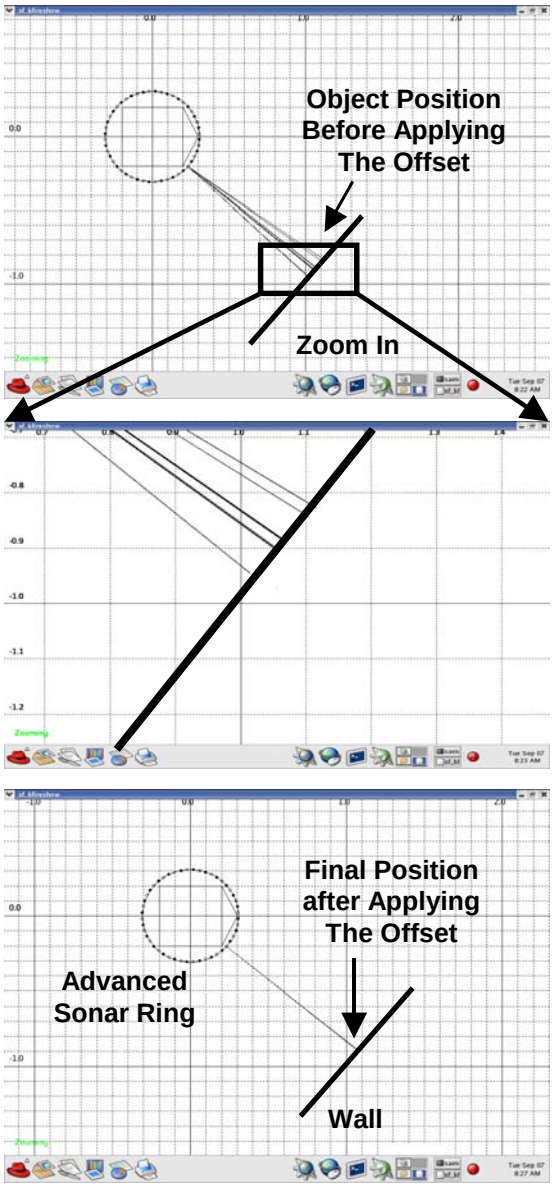


Figure 10. Experimental Result of a Wall position befor and after Applying the Offset

The software uses a lookup table called offset table that contains offset values between the reference template and all others. To calculate the offset value, correlation between each template and the reference template is calculated and when maximum correlation occurs, the difference between two start points is calculated and considered as the offset value of that template ( Figure 9). To get sub-sample resolution the above mentioned interpolation method is also used in offset values computation. The offset table is pre-computed and saved with templates. Using offset values the equation (13) can be rewritten as

$$TOF = 4\mu\sec(pulse\_peak\_no - template\_peak\_no - shift - offset) \quad (21)$$

when the offsets are not applied, the result of range estimation for a stationary target such as a wall is not consistent and different ranges are calculated when the maximum correlation occurs with different templates. The experimental results, before and after applying this factor are shown in Figure 10. This problem also occurs when a calculation process of a moviing platform or moving target uses different templates due to change in the given range, for example when it uses 1 metre templates and then changes to two meter templates. Therefore the offset table increases the robustness of the advanced sonar ring.

## 5.2 Cycle Hopping Rejection Concept and Results

The matched filtering is performed using a 13-point cross correlation, explained in section 3, between a determined echo and each of the related templates for a given range. If the maximum correlation is greater than 80% then the echo is considered as a reliable echo, then the arrival time of the echo is estimated using equation (13).

During experiments, we found the position of a stationary object sometimes jumps between two different positions. More investigation of the echoes showed that the maximum value of the cross correlation, which is sampled at the same rate of the echo, occurs in different locations within cross correlation vector, resulting a varying TOF value caused by a changing shift, described in equation (13). This problem is called cycle hopping since the error in shift is usually approximately one wavelength and details are shown in Figure 11.

The problem arises firstly due to a low sample rate of 250 kHz missing the real peak in the sampling process, and also due to the noise level in the captured echo, which makes local maxima very close to each other and indistinguishable in some conditions. Cycle hopping occurs when the amplitude of an adjacent local maximum is greater than that of the samples calculated around the real peak position.

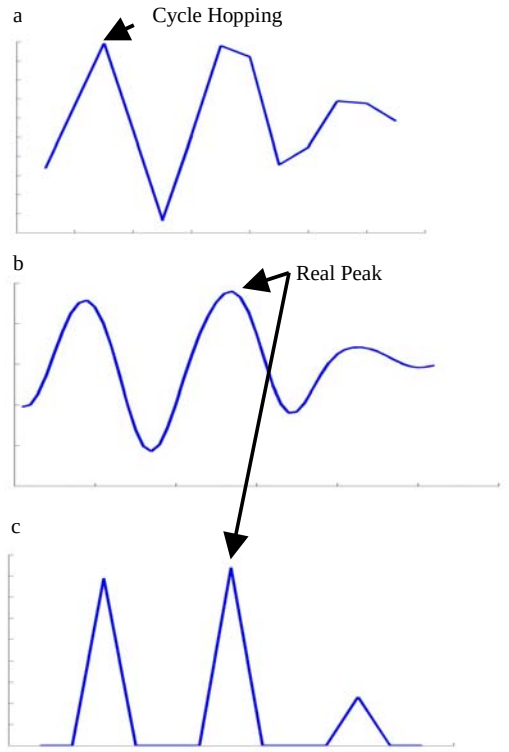


Figure 11. (a) A cross correlation at 250 kHz and the cycle hopping problem (b) the real shape of cross Correlatiom (c) real peak location using the interpolation method

To solve the problem and to find a genuine peak position within the cross correlation matrix, an interpolation process is employed after the cross correlation calculation. This process computes a real peak value of the local maxima using a parabolic interpolation over three adjacent samples. Then, the maximum is chosen amongst the results of this process.

Figure 11 (a) shows a real cross correlation vector which has a peak in the wrong position, comparing to the other echoes captured from the same target and the same receiver. Figure 11 (b) shows the real correlation waveform and the result of the interpolation process on the local maxima is shown in Figure 11 (c). As can be seen, this method can provide a better estimate of the real maximum and avoid the varying TOF.

Also, experimental results are shown in Figure 12. This figure shows the effectiveness of the applied method in the real environment. The computed position of each object is considered at the end of each line. The cycle hopping causes a difference of about 4 samples i.e. 16 microseconds in the arrival time of the echo, therefore about 16*0.343/2=2.75 mm difference in the range. As can be seen in Figure 12, this variation effects the bearing estimation markedly when one of the ranges obtained from a receiver of each pair is fluctuating .

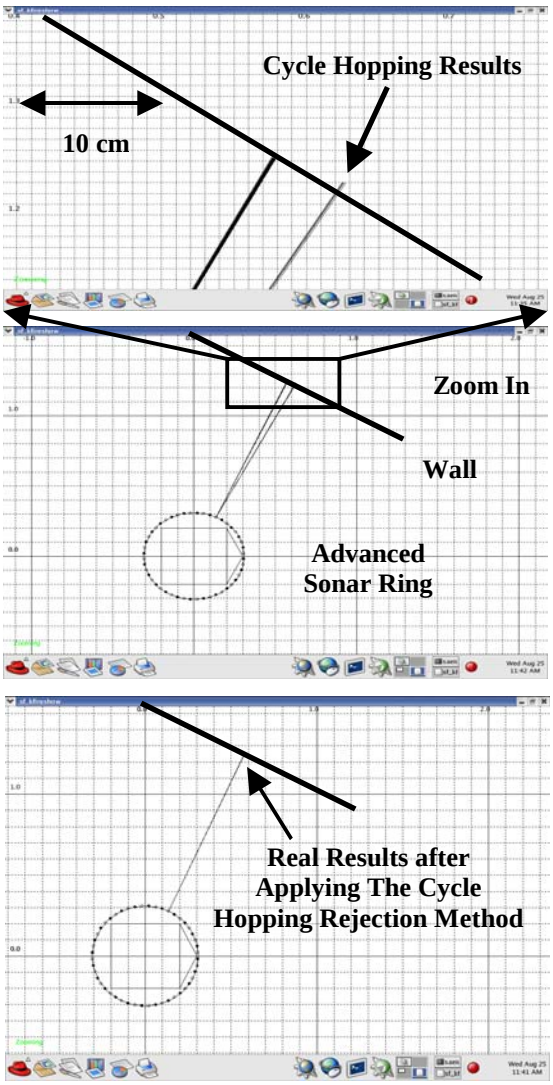


Figure 12. Experimental Data Showing the Effectiveness of The Cycle Hopping Rejection Method

## 6 Conclusions

The paper has presented a new approach to a low sample rate multi DSP real time sonar-ring echo processing based on the template matched arrival time estimator. The concept of a reference point, an offset table and the problem of cycle hopping at the low sample rates has been discussed and the effectiveness of the interpolation solution has been demonstrated with experimental data.

Future work will be performed with high speed accurate sonar sensing applications on a mobile robot such as localization, SLAM, obstacle detection, environmental change detection and path-planning.

## Acknowledgements

We gratefully acknowledge Mr. Steven Armstrong for his assistance in the design and construction of the hardware and basic communication infrastructure of the sonar ring and funding from the ARC Centre for Perceptive and Intelligent Machines in Complex Environments.

## References

[Borenstein, J. and Y. Koren 1995]. "Error eliminating rapid ultrasonic firing for mobile robot obstacle avoidance." *IEEE Transactions on Robotics and Automation* **11**(1): 132-138.

[Fazli, S. and L. Kleeman 2004]. A Real Time Advanced Sonar Ring with Simultaneous Firing. *2004 IEEE/RSJ International Conference on Intelligent Robots and Systems*, 1872-1877, Sendai, Japan.

[Heale, A. and L. Kleeman 2000]. A real time DSP sonar echo processor. *2000 IEEE/RSJ International Conference on Intelligent Robots and Systems, Oct 31-Nov 5 2000*, 1261-1266, Takamatsu, Institute of Electrical and Electronics Engineers Inc.

[Joerg, K.-W. and M. Berg 1998]. Mobile robot sonar sensing with pseudo-random codes. *Proceedings of the 1998 IEEE International Conference on Robotics and Automation. Part 4 (of 4), May 16-20 1998*, 2807-2812, Leuven, Belgium, IEEE, Piscataway, NJ, USA.

[Kleeman, L. 1999]. Fast and accurate sonar trackers using double pulse coding. *1999 IEEE/RSJ International Conference on Intelligent Robots and Systems (IROS'99): Human and Environment Friendly Robots whith High Intelligence and Emotional Quotients', Oct 17-Oct 21 1999*, 1185-1190, Kyongju, South Korea, IEEE, Piscataway, NJ, USA.

[Kleeman, L. and R. Kuc 1995]. "Mobile robot sonar for target localization and classification." *International Journal of Robotics Research* **14**(4): 295-318.

[P.M.Woodward 1964]. *Probability and Information Theory with Application to Radar*, Oxford:Pergamon Press.

[Peremans, H., K. Audenaert, et al. 1993]. "High-resolution sensor based on tri-aural perception." *IEEE Transactions on Robotics and Automation* **9**(1): 36-48.

[Vlastimil MASEK, M. K., Aiguo MING and Ljubisa VLACIC 1998]. "Fast Mobile Robot Obstacle Detection Using Simultaneous Firing of Sonar Ring Sensors."

[Vlastimil MASEK, M. K., Aiguo MING and Ljubisa VLACIC 1999]. "A New Method to Improve Obstacle Detection Accuracy Using Simultaneous Firing of Sonar Ring Sensors." *The Japan Society for Precision Engineering* **33**(N0.1): 49-54.

[Yata, T., A. Ohya, et al. 1999]. "Fast and accurate sonar-ring sensor for a mobile robot." *Proceedings - IEEE International Conference on Robotics and Automation Proceedings of the 1999 IEEE International Conference on Robotics and Automation, ICRA99, May 10-May 15 1999* **1**: 630-636.

[Yata, T., A. Ohya, et al. 2000]. Using one bit wave memory for mobile robots' new sonar-ring sensors. *2000 IEEE International Conference on Systems, Man and Cybernetics, Oct 8-Oct 11 2000*, 3562-3567, Nashville, TN, USA, Institute of Electrical and Electronics Engineers Inc., Piscataway, NJ, USA.